Superlattice Formation in Binary Mixtures of Hard-Sphere Colloids

P. Bartlett,[1] R. H. Ottewill,[1] and P. N. Pusey[2]

[1]*School of Chemistry, Bristol University, Cantock's Close, Bristol, BS8 1TS, United Kingdom*

[2]*Department of Physics, Edinburgh University, Mayfield Road, Edinburgh, EH9 3JZ, United Kingdom*

(Received 11 February 1992)

Binary mixtures of suspended hard-sphere colloidal particles, radius ratio $R_B/R_A=0.58$, were observed to undergo entropically driven freezing transitions into both the AB_2 and the AB_{13} superlattice structures at different relative proportions of the two species. The structures were identified by powder light crystallography and by electron microscopy of the dried solid phases. An approximate (constant volume) phase diagram containing three eutectics was determined. The results are compared with earlier work at size ratio 0.62.

PACS numbers: 82.70.Dd, 61.55.Hg, 64.70.Dv, 81.30.Dz

Remarkably, the first examples of superlattice structures in colloidal crystals were found by Sanders [1] in native gem opals, which consist of dried arrays of colloidal silica spheres. By electron microscopy of a particular sample of Brazilian opal, Sanders observed mixtures of large, A, spheres and small, B, spheres (radii $R_A=181$ nm, $R_B=105$ nm, radius ratio $R_B/R_A\sim0.58$) arranged in both the AB_2 (atomic analogs: borides such as AlB_2) and AB_{13} (atomic analogs: $NaZn_{13}$, UBe_{13}, etc.) structures. Subsequently Yoshimura and Hachisu [2], by direct optical microscopy near the wall of the sample cell, observed at least five different superlattices, including AB_2 and AB_{13}, in a binary suspension of charge-stabilized spheres. However, in neither of these pioneering studies were the conditions required for superlattice formation well characterized. Here we describe the main findings of an experimental investigation of the phase behavior and structure of suspensions of binary mixtures of "hard-sphere" colloidal particles; a more detailed account will be given later. As with the opals the size ratio was about 0.58 and, in regions of the phase diagram whose boundaries were determined reasonably accurately, both the AB_2 and AB_{13} structures were observed. Probably the most interesting implication of these findings is that a system as simple, conceptually, as a mixture of hard spheres can "self-assemble" into quite complex structures, driven purely by entropic (or "packing") contributions to its free energy.

The particles used consisted of polymethylmethacrylate (PMMA) cores, stabilized sterically by thin, ~10 nm, layers of poly-12-hydroxystearic acid [3]. They were suspended in mixtures of decalin and carbon disulphide in proportion chosen to achieve a near match with the refractive index, ~1.5, of the particles, thus providing nearly transparent suspensions suitable for quantitative light scattering studies. One-component suspensions of this type have been studied extensively with emphasis on particle dynamics [4], phase behavior [5], crystallization [6], and glass formation [7]. These studies have established that the interparticle interaction is steep and repulsive and is well approximated by that of hard spheres. We have also reported work [8] on a binary mixture at a slightly larger size ratio, 0.62, which will be compared below with the present research.

The particle radii were determined to be $R_A=321$ nm and $R_B=186$ nm [9]. As in previous work, cited above, particle volume fractions, ϕ_A and ϕ_B, in the suspensions were calculated by scaling the accurately measured weight fractions by factors chosen to ensure that freezing of the individual one-component systems occurred at the hard-sphere value $\phi_A=\phi_B=0.494$. The points in Fig. 1

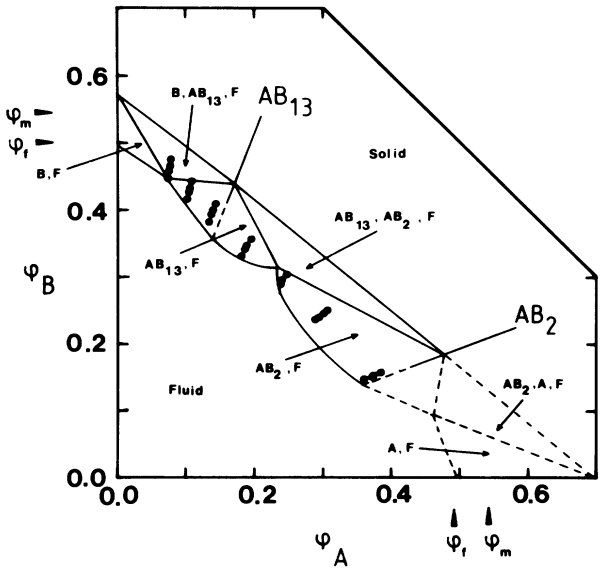

FIG. 1. Constant-volume phase diagram of binary hard-sphere mixtures at size ratio $R_B/R_A=0.58$. The axes are the partial volume fractions ϕ_A and ϕ_B of each species; ϕ_f and ϕ_m indicate the pure-component freezing and melting concentrations. The points show the samples studied. The low-concentration state is fluid. At higher concentrations four regions of coexistence of crystal (B, AB_{13}, AB_2, or A) and fluid (F) are found; the A,F and B,F regions were studied in earlier work [8] at $R_B/R_A=0.62$. The triangles at still higher concentrations are three-phase (two crystals+fluid) eutectic regions and at the highest concentrations, not studied in this work, crystal/crystal coexistence is expected. The two lines radiating from the origin indicate the AB_2 and AB_{13} stoichiometries.

show the samples studied. This representation of the phase diagram, in which the axes are ϕ_A and ϕ_B, is a natural one for colloidal mixtures [10] which (as for colloidal systems in general) are studied at essentially constant volume; lines radiating from the origin correspond to changing the total volume fraction, $\phi_A+\phi_B$, at a fixed ratio, n_B/n_A, of the numbers of the two species. As described elsewhere [11], sedimentation of the particles was minimized by subjecting the samples to "time-averaged zero gravity."

The crystalline structures formed were characterized mainly by "powder light crystallography" [6,8]; an expanded laser beam illuminated many small, randomly oriented crystallites of typical dimension 25 μm. In a few cases the solid phase was also imaged by scanning electron microscopy. The suspension medium was allowed to evaporate over several months. The dried "compact" of colloidal spheres was then fractured and sputter coated with gold in vacuo.

We consider first the AB_2 structure which was observed in suspensions with number ratios n_B/n_A of the species of 4 and 6 and total volume fractions $\phi_A+\phi_B$ between 0.525 and 0.557 (see Fig. 1). About five weeks after preparation the initially homogeneous samples had each separated into a lower solid phase, containing small homogeneously nucleated crystallites, and an upper (colloidal) fluid phase, in differing proportions by volume. Figure 2(a) shows an electron microscope image of the dried solid phase. Long-ranged binary order is clearly visible. The models shown in Fig. 2(b) demonstrate that this and other similar micrographs are consistent with the AB_2 structure which consists of alternating hexagonal

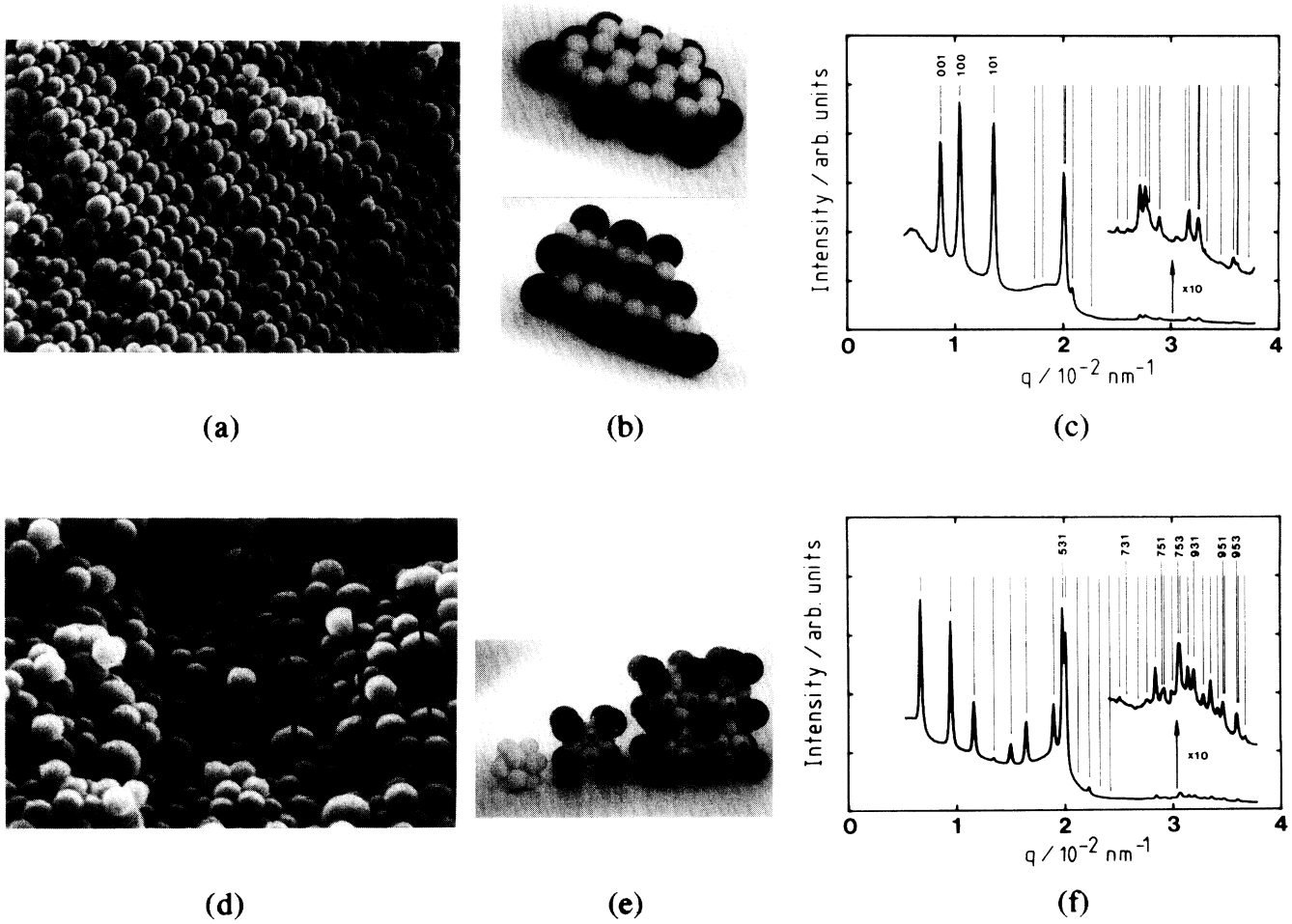

FIG. 2. (a) Electron micrograph of AB_2 superlattice; original composition (OC) of sample $n_B/n_A=6$, $\phi_A+\phi_B=0.536$; (b) model of AB_2; (c) light powder diffraction pattern of AB_2 sample with OC $n_B/n_A=4$, $\phi_A+\phi_B=0.533$; the vertical lines indicate the expected Bragg reflections; (d) micrograph of AB_{13} from sample of OC $n_B/n_A=14$, $\phi_A+\phi_B=0.553$; twelve ordered large spheres are indicated, comprising the 011 face; pentagons of small spheres can be seen below the arrows; (e) model indicating construction of AB_{13}: an icosahedral arrangement of thirteen small spheres, the cubic subcell and the unit cell; two small spheres in each icosahedron are marked to indicate the rotation by $\pi/2$ between subcells; (f) powder pattern of AB_{13} sample with OC $n_A/n_B=9$, $\phi_A+\phi_B=0.552$; the vertical lines indicate the expected reflections; the labeled reflections with odd indices arise from the large unit cell; the unlabeled reflections are those expected for a simple cubic structure but multiplied by 2, i.e., 200, 220, 222, 400, etc.

layers of large and small spheres. The larger A spheres are stacked above one another along the c axis; the smaller B spheres occupy the trigonal prismatic cavities between the A layers. Figure 2(a) can be recognized as showing an approximate 011 section in which the hexagonal layers lie at roughly 45° to the plane of the micrograph; the model in Fig. 2(b) is constructed to also reveal the 011 face.

Figure 2(c) shows a typical powder pattern of one of these samples; the scattered intensity $I(q)$ is plotted against the usual scattering vector q. Quantitative analysis of patterns such as these is complicated by the fact that it is very difficult to measure the form factors of the individual species of particle under conditions of near refractive-index match [8]; thus scattered intensities cannot be calculated easily. However, as is indicated in Fig. 2(c), the experimental and theoretical positions of the Bragg reflections can be compared. Although a few lines are missing (due presumably to destructive interference or minima in the particle form factors), the experimental powder pattern is clearly consistent with the AB_2 structure (space group $P6/mmm$). The rather high background intensity observed at low q probably comprises both scattering from amorphous regions of the solid phase (which were also observed in the electron micrographs) and incoherent scattering associated with a small degree of particle polydispersity [7]. The dimensions of the hexagonal unit cell used to calculate the line positions shown in Fig. 2(c) were $a=693$ nm and $c=724$ nm. The density, $\phi_A+\phi_B=0.64$, of the AB_2 crystal, calculated from these lattice parameters and the particle radii, is considerably larger than that of the suspension from which it crystallizes. Finally we mention that, surprisingly, suspensions prepared with $n_B/n_A=2$ (the AB_2 stoichiometry) did not crystallize over several months, but remained amorphous.

The second superlattice structure, AB_{13}, was found in suspensions rich in small spheres, $n_B/n_A=9$, 14, 20, and 30, with $\phi_A+\phi_B=0.512$–0.553. Crystallization was rapid compared to AB_2; crystallites of AB_{13} were observed within a few days of sample preparation (cf. five weeks for AB_2). The structure of AB_{13} is modeled in Fig. 2(e). It is visualized most easily in terms of a cubic subcell. This contains an icosahedral arrangement of twelve small spheres surrounding an additional small sphere which is itself positioned at the center of a primitive cubic cell of large spheres. The full unit cell consists of eight such subcells stacked so that neighboring icosahedra alternate in orientation by $\pi/2$. Convincing evidence for this remarkably complex structure comes from powder crystallography. A typical powder pattern $I(q)$ is shown in Fig. 2(f). The reflections index on a cubic lattice [$4\leq(h^2+k^2+l^2)\leq 120$] with the space symmetry $Fm\bar{3}c$. The cubic lattice constant is $a=1877$ nm and the calculated density of the AB_{13} crystal is $\phi_A+\phi_B=0.59$ (cf. ~ 0.64 for AB_2). As indicated in Fig. 2(f), the observed reflections separate into two sets with the Miller indices (hkl) either all even or all odd. Two lines in the latter set, 531 (the strongest line observed) and 931, are clearly evident. Symmetry arguments show that *only* scattering from the *alternating* orientational order of the icosahedra within each unit cell contributes to the intensity of these odd labeled reflections. If, for example, the icosahedra were orientationally disordered then the space symmetry would reduce to the simple cubic group $Pm3$ (with a consequent halving of the unit cell dimension) and this set of reflections would be absent. Hence the data of Fig. 2(f) provide strong evidence for the full AB_{13} structure described above.

Electron microscopy of AB_{13} was less successful than that of AB_2. For reasons which are uncertain, the structure appeared to be disrupted on drying and amorphous arrangements of the two species were observed most often. Figure 2(d) shows one of the better micrographs. A reasonably well-ordered arrangement of twelve (marked) large spheres, comprising the 011 face of the structure, is evident. Order among the smaller spheres is still less obvious although pentagons of small spheres, which result from cleavage of the icosahedra, can be seen near the center of the micrograph.

We now consider the consequences of our observations for the form of the equilibrium fluid-solid phase diagram. Our experiments show examples of four stable crystalline phases, A, AB_2, AB_{13}, and B, and in the work reported here we have studied in detail the two-phase regions of fluid/AB_2 and fluid/AB_{13} equilibria. In earlier work [8] on a mixture of spheres of size ratio 0.62 (see below) we investigated the fluid/A and fluid/B equilibria, and established that the small spheres are largely insoluble in a crystal of large spheres and vice versa. This fact, combined with the different symmetries of the superlattices, suggests that the equilibrium phase diagram will contain four regions of fluid/crystal coexistence and three eutectic regions corresponding to the equilibria A/AB_2, AB_2/AB_{13}, and AB_{13}/B. In a constant volume, (ϕ_A,ϕ_B) representation, each eutectic region is described by a triangular three-phase domain with the vertices of the triangle corresponding to the densities of the eutectic fluid and the two coexisting solid phases [10]. Although the exact topology of the phase diagram is still under investigation, we can estimate the positions of two of the three eutectic fluids. In particular, the observation of AB_2 formation in suspensions of compositions $n_B/n_A=6$ but AB_{13} formation at compositions $n_B/n_A=9$ and above indicates that the AB_2/AB_{13} eutectic fluid lies at a stoichiometry with n_B/n_A between 6 and 9. Furthermore the position of the AB_{13}/B eutectic is indicated by the experimental observation of three phase equilibria in samples of composition $n_B/n_A=30$ and concentration $\phi_A+\phi_B=0.54-0.56$. Such samples contain two crystalline phases, AB_{13} and B (identified by powder diffraction), together with a single isotropic fluid. Approximate phase boundaries implied by

these observations are sketched in Fig. 1; the right-hand side of the diagram is uncertain because, as mentioned above, suspensions with $n_B/n_A=2$ showed no observable crystallization in our experiments.

Our previous work [8] involved a binary mixture at size ratio $R_B/R_A=0.62$, in which the A spheres were the same, $R_A=321$ nm, but the B spheres had $R_B=199$ nm, cf. 186 nm in the present study. In this mixture we never observed crystalline AB_2; samples with $2<n_B/n_A<10$ remained amorphous over the many months duration of the experiments. Around $n_B/n_A=13$ AB_{13} was observed, but appeared to be metastable: It formed much more slowly than at size ratio 0.58, seemed to "redissolve" after many months, and was always found to be mixed with crystals of pure B. (It seems remarkable that changing the size of one species by just 7% should have such profound effects.)

Discussing these findings, we note first that, following initial vigorous debate, the existence of an entropically driven freezing transition in a *one-component* assembly of hard spheres (which, of course, have no attractive part in their pair potential) is nowadays accepted [5,6,12]. Freezing occurs at a concentration at which the loss of the system's entropy associated with the formation of long-ranged order is more than offset by the gain in entropy associated with the extra free volume available to the spheres in an ordered spatial arrangement [12]. One can expect similar principles to apply to the freezing of binary hard-sphere mixtures. Eldridge and Madden [13] have recently calculated by computer simulation the free energy of AB_{13}. In reasonable agreement with our observations, they find stability of AB_{13} (compared to colloidal fluid and phase-separated crystalline A and B) over a significant range of concentration for $R_B/R_A=0.58$ and instability for $R_B/R_A>0.62$. Simulations of AB_2 are in progress [13]. Approximate calculations based on estimating free volume give similar results for AB_{13} and also suggest that AB_2 should be stable at $R_B/R_A=0.58$ [14].

Intriguing, as yet unexplained, observations include the facts that the complex AB_{13} structure grew significantly faster than AB_2 and that AB_2 itself grew fastest from a metastable fluid at the $n_B/n_A=6$ stoichiometry (close to the AB_2/AB_{13} eutectic, see above) and not at all at $n_B/n_A=2$. The latter is surprising since glass formation is usually expected near to a eutectic rather than at the stoichiometry of a crystalline compound [15].

It is clear that purely entropic contributions to the free energies of simple systems can lead to the formation of complex structures. Obvious future directions include more detailed studies of the kinetics and mechanisms of superlattice formation and of the binary glass transitions, and the possibility of fabricating new materials by mixing, for example, plastic and metallic or semiconductor particles of different sizes.

We thank M. D. Eldridge and P. A. Madden for communicating their results prior to publication. This research was supported by a joint grant from the Science and Engineering Research Council and the Ministry of Defense, and was performed in part while P.N.P. was at the Royal Signals and Radar Establishment, Malvern, United Kingdom.

[1] J. V. Sanders, Philos. Mag. A **42**, 705 (1980).
[2] S. Yoshimura and S. Hachisu, Prog. Colloid Polym. Sci. **68**, 59 (1983).
[3] L. Antl, J. W. Goodwin, R. D. Hill, R. H. Ottewill, S. M. Owens, S. Papworth, and J. A. Waters, Colloid Surf. **17**, 67 (1986).
[4] P. N. Pusey and W. van Megen, J. Phys. (Paris) **44**, 285 (1983); W. van Megen and S. M. Underwood, Langmuir **6**, 35 (1990).
[5] P. N. Pusey and W. van Megen, Nature (London) **320**, 340 (1986); S. E. Paulin and B. J. Ackerson, Phys. Rev. Lett. **64**, 2663 (1990).
[6] P. N. Pusey, W. van Megen, P. Bartlett, B. J. Ackerson, J. G. Rarity, and S. M. Underwood, Phys. Rev. Lett. **63**, 2753 (1989).
[7] W. van Megen and P. N. Pusey, Phys. Rev. A **43**, 5429 (1991); W. van Megen, S. M. Underwood, and P. N. Pusey, Phys. Rev. Lett. **67**, 1586 (1991).
[8] P. Bartlett, R. H. Ottewill, and P. N. Pusey, J. Chem. Phys. **93**, 1299 (1990).
[9] These radii were calculated from the expression $\phi=\frac{4}{3}\pi R^3\rho$, the number density ρ being obtained from the measured lattice parameters of the one-component crystals at melting (volume fraction $\phi=\phi_M=0.545$ for hard spheres). This approach leads to a size ratio of 0.62 for the system described in Ref. [8], rather than the value 0.61 quoted there.
[10] P. Bartlett, J. Phys. Condens. Matter **2**, 4979 (1990).
[11] P. Bartlett, P. N. Pusey, and R. H. Ottewill, Langmuir **7**, 213 (1991).
[12] For a recent discussion, see H. N. W. Lekkerkerker, in *Phase Transitions in Soft Condensed Matter*, edited by T. Riste and D. Sherrington (Plenum, New York, 1989), p. 165.
[13] M. D. Eldridge and P. A. Madden (to be published); (private communication).
[14] P. Bartlett (unpublished).
[15] F. Spaepen and D. Turnbull, Annu. Rev. Phys. Chem. **35**, 241 (1984).

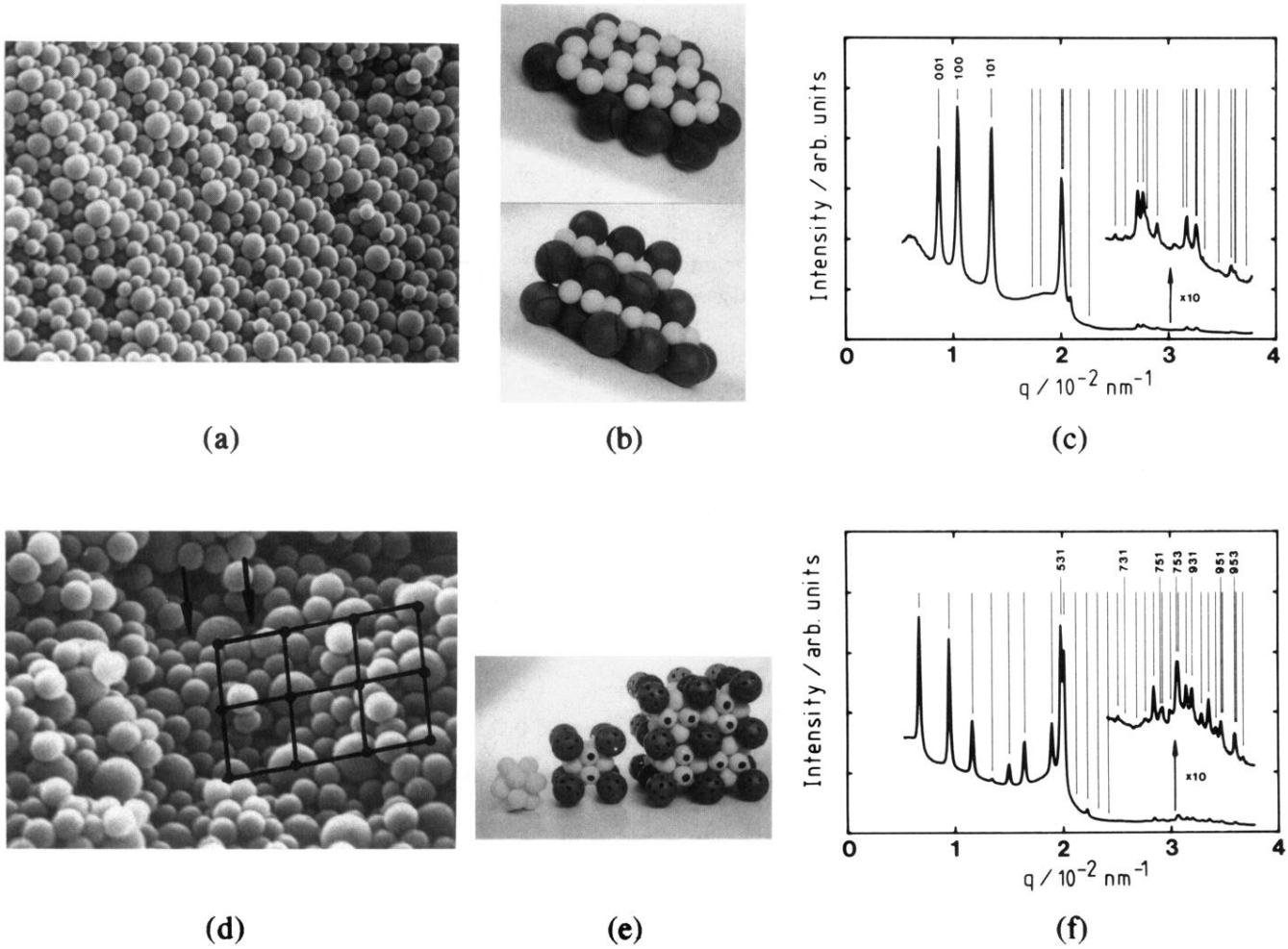

FIG. 2. (a) Electron micrograph of AB_2 superlattice; original composition (OC) of sample $n_B/n_A=6$, $\phi_A+\phi_B=0.536$; (b) model of AB_2; (c) light powder diffraction pattern of AB_2 sample with OC $n_B/n_A=4$, $\phi_A+\phi_B=0.533$; the vertical lines indicate the expected Bragg reflections; (d) micrograph of AB_{13} from sample of OC $n_B/n_A=14$, $\phi_A+\phi_B=0.553$; twelve ordered large spheres are indicated, comprising the 011 face; pentagons of small spheres can be seen below the arrows; (e) model indicating construction of AB_{13}: an icosahedral arrangement of thirteen small spheres, the cubic subcell and the unit cell; two small spheres in each icosahedron are marked to indicate the rotation by $\pi/2$ between subcells; (f) powder pattern of AB_{13} sample with OC $n_A/n_B=9$, $\phi_A+\phi_B=0.552$; the vertical lines indicate the expected reflections; the labeled reflections with odd indices arise from the large unit cell; the unlabeled reflections are those expected for a simple cubic structure but multiplied by 2, i.e., 200, 220, 222, 400, etc.